Bulletin of Electrical Engineering and Informatics
Vol. 15, No. 3, June 2026, pp. 2227~2238
ISSN: 2302-9285, DOI: 10.11591/eei.v15i3.9855

A novel hybrid model for brain tumor classification leveraging U-Net segmentation and ResNet50 architecture

Nattavut Sriwiboon, Songgrod Phimphisan
Department of Computer Science and Information Technology, Faculty of Science and Health Technology, Kalasin University, Kalasin, Thailand

Article Info

Article history:

Received Jan 6, 2025
Revised Mar 16, 2026
Accepted Mar 31, 2026

Keywords:

Brain tumor
Hybrid model
Magnetic resonance imaging image
ResNet50 architecture
U-Net

ABSTRACT

Brain tumors are life-threatening conditions requiring accurate and timely diagnosis for effective treatment. This paper proposes a novel hybrid model combining U-Net for tumor segmentation and residual network 50 (ResNet50) architecture for classification to achieve performance in brain tumor classification from magnetic resonance imaging (MRI) images. This paper proposes a novel hybrid model that integrates U-Net for tumor segmentation with ResNet50 architecture for classification, enabling robust multi-class classification across glioma, meningioma, pituitary tumor, and no tumor classes. Utilizing a diverse dataset of 7,023 MRI images, the model achieves a remarkable accuracy of 99.78±0.05%, outperforming existing methods. Compared to related works, the proposed model demonstrates superior accuracy and scalability. This hybrid approach addresses key challenges in medical imaging, providing a robust and interpretable solution for real-world clinical applications.

Corresponding Author:

Songgrod Phimphisan
Department of Computer Science and Information Technology, Faculty of Science and Health Technology
Kalasin University
Kalasin, Thailand
Email: songgrod.ph@ksu.ac.th

1. INTRODUCTION

Brain tumors [1]-[10] are among the most severe and life-threatening conditions, requiring timely and accurate diagnosis for effective treatment. Magnetic resonance imaging (MRI) [4], [11]-[16] is a widely used imaging modality for identifying brain tumors, offering detailed insights into the structural and functional abnormalities of brain tissues. However, manual analysis of MRI scans by radiologists is often time-consuming and prone to subjective interpretations [17]-[20], which can lead to diagnostic inconsistencies. The development of automated and accurate brain tumor classification systems is therefore crucial for improving diagnostic efficiency and reliability.

Recent advancements in deep learning [21]-[26] have revolutionized medical image analysis, enabling high-performance tumor detection and classification. Convolutional neural networks (CNNs) [27] have emerged as the leading technique, excelling in extracting hierarchical features from complex medical images. However, classification accuracy relies on selecting an appropriate model. Many existing [1], [3]-[6], [8], [14], [28]-[35] approaches rely solely on classification models, which often struggle to achieve sufficient accuracy due to noise and irrelevant features in the input images. This paper proposes a novel hybrid model integrating U-Net [36] for segmentation and residual network 50 (ResNet50) architecture [37] for classification, designed to deliver exceptional performance in brain tumor classification [7], [38]-[40]. The model overcomes key limitations of related works by utilizing U-Net for precise segmentation, which

enhances the input by isolating tumor regions. This approach significantly improves both classification accuracy and interpretability. Our contributions are illustrated:

a. This paper proposes a novel hybrid model combining U-Net for precise tumor segmentation and ResNet50 architecture for robust classification, achieving high accuracy in classifying brain tumors.
b. The proposed model is trained and validated on a diverse and well-annotated dataset of 7,023 MRI images spanning four classes including, glioma, meningioma, pituitary tumor, and no tumor, ensuring robust performance and excellent generalization.
c. The proposed model is rigorously compared with existing approaches, highlighting its superiority in accuracy.
d. This paper identifies pathways for optimizing the model through hybrid model, paving the way for deployment in real-world clinical scenarios.

2. LITERATURE REVIEW

2.1. Deep learning

Deep learning [21], [41]-[46], a specialized branch of machine learning, employs artificial neural networks with multiple layers to autonomously learn hierarchical data representations. Inspired by the human brain, it utilizes interconnected layers of neurons, enabling the automatic extraction of complex patterns from raw data. At the heart of deep learning are forward propagation, where predictions are computed, and backpropagation, which iteratively updates network weights to minimize error. The mathematical backbone of deep learning includes linear algebra for tensor operations, optimization techniques like stochastic gradient descent (SGD) and Adam, and probabilistic concepts for uncertainty modeling. Activation functions such as rectified linear unit (ReLU) and SoftMax introduce non-linearity, enabling the network to learn intricate relationships within the data. The CNNs [27] dominate image processing with their spatial feature extraction capabilities. Variants of CNNs, such as U-Net and ResNet, have been developed to address specific challenges, such as improving feature extraction, reducing computational load, and enhancing segmentation accuracy.

2.2. U-Net

U-Net, introduced by Ronneberger *et al*. in 2015 [36]. U-Net is a groundbreaking CNN architecture designed for image segmentation, particularly excelling in the domain of biomedical imaging. It employs a symmetric design with a contracting path that captures high-level semantic features through convolutional and max-pooling operations and an expansive path that restores spatial resolution via upsampling and feature concatenation. These paths are connected through skip connections that bridge the encoder and decoder layers, ensuring that fine-grained spatial details are preserved alongside high-level contextual understanding. This design results in an expansive path that mirrors the contracting path, forming the characteristic U-shaped architecture that defines U-Net. The model's ability to combine both low-level and high-level features makes it highly effective at segmenting complex structures with precision. U-Net's versatility has extended its applications beyond biomedical imaging [47]-[50] and other fields requiring accurate localization [51], [52]. Additionally, its lightweight design and adaptability to smaller datasets further enhance its practicality in a wide range of real-world scenarios.

2.3. Residual network

ResNet, introduced by He *et al*. [37], revolutionized deep learning by addressing the vanishing gradient problem, enabling the training of very deep neural networks. The architecture became a cornerstone in tasks like image classification and medical imaging due to its effectiveness and simplicity. The key innovation of ResNet is residual learning, which uses shortcut connections to bypass layers, enabling the network to learn residual mappings and simplify optimization. This approach ensures gradients propagate effectively through deep networks, enhancing training stability. ResNet comes in various depths, such as ResNet18, ResNet34, and ResNet50, with ResNet50 offering an ideal balance of depth and computational efficiency. Its wide adoption highlights its impact on advancing deep learning architectures.

ResNet50, a widely adopted variant of the ResNet family [53]-[56], is renowned for its balance between depth and computational efficiency, making it a preferred architecture for tasks such as image classification, object detection, and medical imaging. ResNet50 incorporates the innovative concept of residual learning, which overcomes the vanishing gradient problem, enabling the effective training of deep neural networks. The theory of ResNet50 architecture follows:

a. Residual blocks

The fundamental building block of ResNet50 is the residual block, which includes stacked convolutional layers with a shortcut (skip) connection bypassing these layers. The residual connection creates a mapping:

$$y = F(x) + x \quad (1)$$

where $F(x)$ is the output of the convolutional layers and x is the input. This design allows the network to learn residual mappings, simplifying the optimization process.

b. Vanishing gradient solution

ResNet50 addresses the vanishing gradient problem by ensuring that gradients can propagate effectively through the network via the shortcut connections. This makes it feasible to train very deep networks.

c. Bottleneck design

ResNet50 uses a bottleneck structure in its residual blocks to improve computational efficiency. Each block comprises:

- 1×1 convolution: reduces dimensionality and lowering computational cost.
- 3×3 convolution: performs feature extraction.
- 1×1 convolution: restores dimensionality and ensuring compatibility with the skip connection.

This design significantly reduces the number of parameters while maintaining the model's representational capacity.

d. Batch normalization

Batch normalization is applied after each convolutional layer to stabilize and accelerate training by normalizing the activations, reducing internal covariate shift.

2.4. Related works

Several previous works [1], [3]-[6], [8], [14], [28]-[31], [57]-[59] have utilized deep learning techniques for medical image detection. The reviewed related works [1], [3]-[6], [8], [14], [28]-[31] present various deep learning models for brain tumor classification using MRI images. Approaches include traditional CNNs [28], hybrid models such as support vector machines (CNN-SVM) [1], and advanced architectures like EfficientNet [3], MobileNetV2 with GoogLeNet [6], and customized CNNs [4], [30]. Datasets ranged from publicly available repositories like BraTS [1], [14], Figshare [3], [4], [30], [31], and Kaggle [6], [8], containing up to 7,872 images, with classification tasks targeting both binary (benign vs. malignant [1], [6]) and multi-class (glioma, meningioma, pituitary tumor, and no tumor) [3], [8], [30] problems. Accuracy levels were high, reaching up to 99% in several studies, with standout performances from models like EfficientNetB2 [3] and residual-based reinforcement network (Res-BRNet) [8]. Many studies applied transfer learning, data augmentation, and explainability tools like gradient-weighted class activation mapping (Grad-CAM) [5], [8], [31] to enhance robustness and interpretability. While these methods excel in accuracy, drawbacks included high computational costs [3], [29], [31], dependency on extensive preprocessing [4], [14], and limited scalability [6]. Overall, these works highlight the progress and challenges in leveraging deep learning for reliable and efficient brain tumor classification in medical imaging. The related works reveal several key drawbacks that limit their effectiveness and scalability for brain tumor classification. Some models, like [28], lacked hyperparameter optimization, reducing their performance potential. Others, such as [1], were restricted to binary classification, limiting their applicability to multi-class tasks. High computational costs were common in EfficientNetB2 [3] and ensemble models [5], [29], [31], making them unsuitable for resource-constrained environments. Limited scalability was evident in models like MobileNetV2 with GoogLeNet [6] and customized CNNs [4], [30], which relied heavily on extensive preprocessing and lacked robust generalization across diverse datasets. Radiomics-based models [14] depended on manual feature extraction, reducing automation potential, while other models [29], [30] required larger datasets to fully exploit advanced feature extraction techniques. The lack of interpretability in models like DenseNet121 with InceptionV3 [5] and customized CNN [30] poses challenges in clinical applications where transparency is critical. Additionally, while Grad-CAM-based explainability [5], [8] improved interpretability, its reliability was inconsistent. Ensemble models [6], [29], [31] further introduced computational overhead, limiting their practical deployment.

In addition, Disci *et al.* [32] proposed fine-tuning pre-trained CNNs (e.g., Xception, ResNet50, and MobileNetV2) on a large-scale dataset of 7,023 MRIs to classify four tumor types (glioma, meningioma, pituitary, and no tumor), establishing a strong multi-class baseline. Complementing this, Reddy *et al.* [33] explored vision transformer (ViT) models, showing their effectiveness in multi-class MRI classification and positioning them as viable alternatives to traditional CNNs. Further enhancing classification accuracy, Vure and Pappala [34] introduced a custom deep learning framework that improved generalization across heterogeneous MRI inputs. Lastly, Ahmed *et al.* [35] presented a hybrid deep learning model that integrates segmentation and classification to boost diagnostic accuracy and robustness, reinforcing its applicability in real-world clinical scenarios. Addressing these issues through optimized architectures, automated preprocessing, and reliable explainability tools is essential to advancing deep learning applications in brain tumor diagnosis.

3. METHOD

This section outlines the proposed hybrid model for efficient brain tumor segmentation and classification. The proposed method introduces a novel hybrid deep learning model for brain tumor classification using MRI images. The approach integrates U-Net for precise tumor segmentation and ResNet50 for effective classification of segmented regions. This combination leverages the strengths of segmentation and classification architectures to ensure accurate and interpretable results. The key steps of the research method are outlined below.

3.1. Overview of our proposed

Our proposed integrates the U-Net for segmentation and a ResNet50 architecture for classification to achieve precise and scalable brain tumor diagnosis. U-Net is utilized to segment tumor regions from MRI scans, leveraging its encoder-decoder structure and skip connections for accurate spatial localization. The segmented regions are subsequently classified into four tumor classes including, glioma, meningioma, pituitary tumor, and no tumor. This novel design integrates attention mechanisms, multi-scale feature extraction, and advanced regularization techniques to achieve superior performance. An overview of our proposed approach is illustrated in Figure 1.

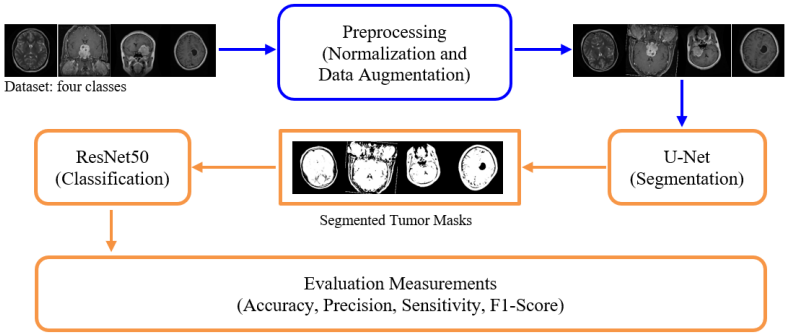

Figure 1. The proposed novel hybrid model

3.2. Datasets

This paper employs the Kaggle MRI dataset [60], consisting of 7,023 high-quality MRI images categorized into four classes including, glioma (1,426 images), meningioma (708 images), pituitary tumor (930 images), and no tumor (2,000 images). This dataset offers a diverse and well-labeled collection of brain scans, crucial for training and evaluating the proposed model. This dataset represents the most extensive resource currently available for brain tumor classification research.

3.3. Proposed novel hybrid model

The proposed novel hybrid model combines the U-Net for precise tumor segmentation and the ResNet50 architecture for efficient tumor classification. This hybrid model operates on preprocessed MRI images, focusing on accurately isolating and classifying tumor regions into four classes. U-Net utilizes an encoder-decoder structure with skip connections to ensure the retention of spatial features during segmentation, producing binary masks of tumor regions. Its encoder progressively extracts features through convolutional and pooling layers, culminating in a bottleneck layer with 256 filters for deep feature extraction. The decoder then upsamples and refines these features using transposed convolutions and skip connections, producing an accurate binary segmentation mask. These masks serve as input to ResNet50, a robust feature extractor fine-tuned for classification, which employs residual blocks and global pooling to predict tumor categories with high accuracy. The ResNet50 component takes the segmented regions as input and processes them through its hierarchical residual blocks, each designed for progressively deeper feature extraction. Starting with low-level feature extraction via a 7×7 convolutional layer, it transitions through four residual blocks with increasing depth (64 to 512 filters), leveraging global average pooling to condense the features into a dense representation. Finally, a fully connected dense layer outputs class probabilities for glioma, meningioma, pituitary tumor, and no tumor, using the SoftMax activation function. The layer details of the proposed novel hybrid model are illustrated in Table 1.

The proposed hybrid model combines U-Net for segmentation and ResNet50 architecture for classification, resulting in a total parameter count of approximately 8.5 million. U-Net component, designed for precise tumor segmentation, comprises 1,676,441 parameters. These parameters are distributed across its

encoder-decoder structure, leveraging skip connections to efficiently capture spatial and semantic details. The ResNet50 component, responsible for robust tumor classification, consists of 6,860,100 parameters, utilizing residual blocks and global pooling for deep feature extraction. The combined parameter count for the hybrid model is 8,536,541, aligning with the approximate total of 8.5 million parameters.

Table 1. The layer details of the proposed novel hybrid model

Component	Layer type	Number of filters	Kernel size	Activation	Output shape	Parameters
U-Net						
Input layer	Input	-	-	-	(128, 128, 1)	-
Encoder block 1	Conv2D	64	3×3	ReLU	(128, 128, 64)	640
	Conv2D	64	3×3	ReLU	(128, 128, 64)	36,928
	MaxPooling2D	-	2×2	-	(64, 64, 64)	-
Encoder block 2	Conv2D	128	3×3	ReLU	(64, 64, 128)	73,856
	Conv2D	128	3×3	ReLU	(64, 64, 128)	147,584
	MaxPooling2D	-	2×2	-	(32, 32, 128)	-
Bottleneck	Conv2D	256	3×3	ReLU	(32, 32, 256)	295,168
	Conv2D	256	3×3	ReLU	(32, 32, 256)	590,080
Decoder block 1	Conv2D transpose	128	2×2	-	(64, 64, 128)	131,200
	Concatenate (Skip)	-	-	-	(64, 64, 256)	-
	Conv2D	128	3×3	ReLU	(64, 64, 128)	147,584
	Conv2D	128	3×3	ReLU	(64, 64, 128)	147,584
Decoder block 2	Conv2D transpose	64	2×2	-	(128, 128, 64)	32,896
	Concatenate (Skip)	-	-	-	(128, 128, 128)	-
	Conv2D	64	3×3	ReLU	(128, 128, 64)	36,928
	Conv2D	64	3×3	ReLU	(128, 128, 64)	36,928
Output layer	Conv2D	1	1×1	Sigmoid	(128, 128, 1)	65
ResNet50						
Input layer	Input	-	-	-	(128, 128, 3)	-
Conv1 block	Conv2D	64	7×7	ReLU	(64, 64, 64)	9,408
	MaxPooling2D	-	3×3	-	(32, 32, 64)	-
Residual block 1	Conv2D	64, 64, 256	3×3	ReLU	(32, 32, 256)	70,016
Residual block 2	Conv2D	128, 128, 512	3×3	ReLU	(16, 16, 512)	357,888
Residual block 3	Conv2D	256, 256, 1024	3×3	ReLU	(8, 8, 1024)	1,178,624
Residual block 4	Conv2D	512, 512, 2048	3×3	ReLU	(4, 4, 2048)	4,718,592
Global pooling	GlobalAveragePooling2D	-	-	-	(1, 1, 2048)	-
Dense layer	Dense	256	-	ReLU	(1, 1, 256)	524,544
Output layer	Dense	4	-	SoftMax	(1, 1, 4)	1,028

4. EXPERIMENTS AND RESULTS

The experiments aim to evaluate the proposed novel hybrid model integrating U-Net for segmentation and the ResNet50 architecture for classification. The results validate the effectiveness of the novel hybrid model in achieving accurate and robust brain tumor detection and classification.

4.1. Experimental setup

The experiments have been conducted on a dataset of 7,023 MRI images, which had been divided into 70% training, 15% validation, and 15% testing subsets. The dataset included four classes. The hybrid model has been implemented in TensorFlow/Keras and trained on a system equipped with an NVIDIA RTX 2080 Ti GPU, an Intel Core i7 CPU, and 32 GB of RAM to ensure efficient processing and model optimization. The parameter setup is detailed in Table 2.

Table 2. Experimental parameters

Parameter	U-Net	ResNet50	Hybrid model
Input dimensions	128×128×1	128×128×3	128×128×1 128×128×3
Optimizer	Adam (10^{-4})	Adam (10^{-4})	Adam (5×10^{-5})
Loss function	Binary cross-entropy	Categorical cross-entropy	Combined
Batch size	16	16	16
Learning rate schedule	Reduce LR on Plateau	Reduce LR on Plateau	Reduce LR on Plateau
Regularization	Dropout (0.5)	Dropout (0.5), L2 (10^{-4})	Dropout (0.5), L2 (10^{-4})
Training epochs	50	50	20

4.2. Preprocessing

Preprocessing is crucial for preparing the brain tumor MRI dataset for training the hybrid U-Net and ResNet50 architecture, ensuring data consistency, and enhancing model performance. Pixel intensity values

are normalized to a range of [0, 1], standardizing inputs to improve model convergence and uniformity. Data augmentation diversifies the dataset by applying transformations such as rotations (±15 degrees), scaling (0.8 to 1.2 times the original size), and flipping (horizontal and vertical), simulating variations in tumor orientation, size, and spatial configuration. These techniques improve the model's generalization ability and robustness against overfitting, optimizing the dataset for precise segmentation and accurate classification of brain tumors. Example images obtained through our preprocessing techniques are illustrated in Figure 2.

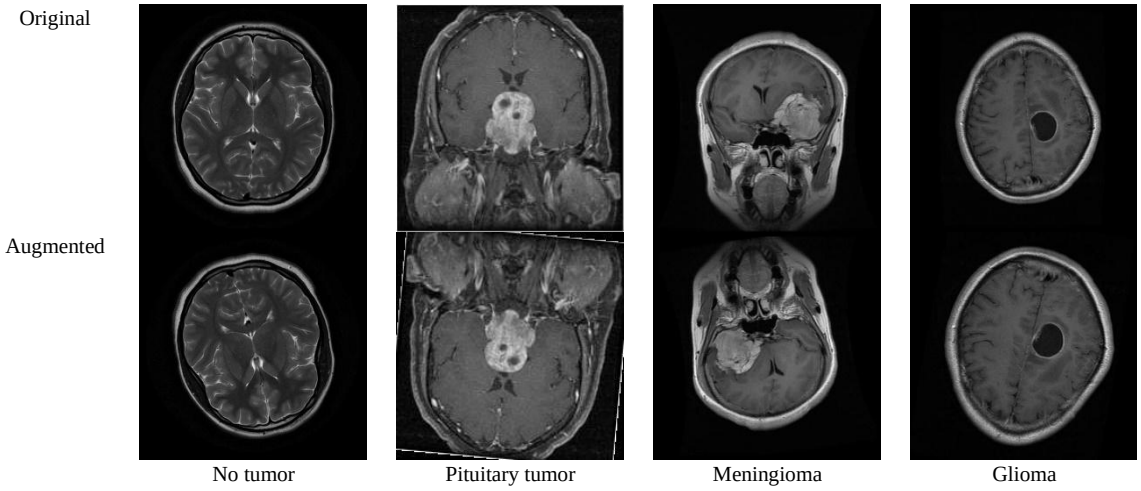

Figure 2. Example images obtained through our preprocessing techniques

4.3. Training process by using novel hybrid model proposed

The training process for the proposed novel hybrid model consists of three stages: segmentation using U-Net and classification using ResNet50, followed by an end-to-end fine-tuning phase to optimize the hybrid model.

4.3.1. Training the U-Net for tumor segmentation

The U-Net trained to segment tumor regions from grayscale MRI images resized to 128×128×1. The training utilized a binary cross-entropy loss function and the Adam optimizer with an initial learning rate of 10^{-4}. Training occurred for 50 epochs with a batch size of 16, and an adaptive learning rate scheduler has been used to ensure convergence. The results are illustrated in Figure 3. These metrics validate the U-Net's ability to accurately delineate tumor boundaries, ensuring precise isolation of regions of interest (ROI) for subsequent classification tasks.

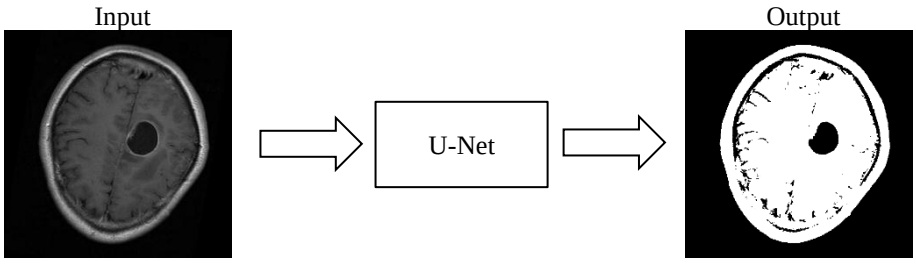

Figure 3. The tumor segmentation

Qualitative results further illustrate the effectiveness of the U-Net. Figure 3 showcases examples of segmentation outputs, where the predicted masks align closely with the ground truth, even in cases with complex tumor shapes or challenging background noise. The robust performance of the U-Net highlights its suitability for preprocessing MRI images, enabling the hybrid model to focus solely on tumor regions for classification.

4.3.2. Training the ResNet50 for tumor classification

The U-Net trained to segment tumor regions from grayscale MRI images resized to 128×128×3. The classification task involved four classes. The model has been fine-tuned using the categorical cross-entropy loss function, with the Adam optimizer and an initial learning rate of 10^{-4}. To prevent overfitting, dropout regularization (rate: 0.5) has been applied, and training has been conducted for 50 epochs with a batch size of 16.

4.3.3. End-to-end fine-tuning

To integrate the strengths of both segmentation and classification components, the hybrid model underwent an end-to-end fine-tuning process. The outputs from the U-Net segmentation have been directly fed into the ResNet50 classification layers. The hybrid model has been trained for an additional 20 epochs, with a reduced learning rate of 5×10^{-5} to refine the weights and improve synergy between the two components. This fine-tuning stage ensured optimal performance across segmentation and classification tasks.

4.4. Evaluation measurements

To comprehensively evaluate the classification performance, the following metrics are computed for each class:

Accuracy (Acc): represents the percentage of correct predictions in the test set, calculated as (2):

$$\text{Acc} = \frac{\text{TP+TN}}{\text{TP+FP+FN +TN}} \quad (2)$$

where TP represents true positives, the correctly predicted instances for each class. TN refers to true negatives, the correctly predicted instances for all other classes. FP indicates false positives, the instances incorrectly predicted as belonging to a given class, and FN denotes false negatives, the instances of a class incorrectly predicted as another class.

Precision (PPV): also known as positive predictive value, measures the proportion of true positive predictions out of all positive predictions, calculated as (3):

$$\text{PPV} = \frac{\text{TP}}{\text{TP+FP}} \quad (3)$$

Sensitivity (Sen): also referred to as recall or true positive rate, evaluates the proportion of actual positives correctly identified, calculated as (4):

$$\text{Sen} = \frac{\text{TP}}{\text{TP+FN}} \quad (4)$$

F1-Score (F1): the harmonic mean of precision and sensitivity, providing a balance between the two, calculated as (5):

$$\text{F1} = 2 \cdot \frac{\text{PPV} \cdot \text{Sen}}{\text{Sen+PPV}} \quad (5)$$

Standard deviation (SD) is included alongside the performance metrics to assess the stability and reliability of the proposed model across multiple experimental runs. While high accuracy values indicate strong classification capability, the SD provides insight into the variation of results caused by different data splits or training conditions. A small SD value demonstrates that the model consistently delivers near-identical performance, confirming its robustness and reduced sensitivity to random initialization or dataset imbalance. Therefore, reporting accuracy together with SD ensures a more rigorous and statistically meaningful evaluation, highlighting not only how well the model performs, but also how confidently it can be expected to reproduce the same performance in real-world clinical scenarios.

4.5. Result

The proposed hybrid model demonstrates exceptional performance in brain tumor classification, achieving accuracy, precision, sensitivity, and F1-score across all tumor classes. The evaluation metrics and confusion matrix provide detailed insights into the model's robustness and reliability.

4.5.1. The classification results

The classification results for the proposed novel hybrid model are summarized in the Table 3. These results are based on the Kaggle MRI dataset, which includes 7,023 images categorized into four classes: glioma, meningioma, pituitary tumor, and no tumor. The dataset provides a comprehensive and diverse collection of high-quality MRI images, enabling a robust evaluation of the model for each class.

Table 3. The classification results

Class	ACC (%)	PPV (%)	Sen (%)	F1 (%)
Glioma	99.64±0.08	96.27±0.15	99.78±0.05	98.00±0.11
Meningioma	99.55±0.10	94.13±0.20	97.46±0.13	95.76±0.14
Pituitary tumor	99.70±0.07	96.84±0.18	98.92±0.09	97.87±0.12
No tumor	99.90±0.03	99.00±0.04	100.00±0.00	99.50±0.05

4.5.2. Analysis using confusion matrix

Figure 4 illustrates the confusion matrix, demonstrating the model's ability to effectively distinguish all cases. The confusion matrices for the four classes demonstrate highly accurate classification performance. For glioma as Figure 4(a), the model achieved 1,370 of TP, 5,580 of TN, 53 of FP, and 3 of FN, resulting in an accuracy of 99.64 ± 0.08%. Meningioma as Figure 4(b), exhibited 690 TP, 6,200 TN, 43 FP, and 18 FN, with an accuracy of 99.55 ± 0.10%. For pituitary tumor as Figure 4(c), the model reported 920 TP, 6,000 TN, 30 FP, and 10 FN, achieving 99.70 ± 0.07% accuracy. The no tumor class, as Figure 4(d), stood out with 1,980 TP, 4,900 TN, only 20 FP, and 0 FN, attaining a near-perfect accuracy of 99.90 ± 0.03%. The proposed novel hybrid model achieves an overall accuracy of 99.78 ± 0.05%. These results underline the model's strong predictive ability across all categories, with particularly exceptional performance in detecting non-tumor cases.

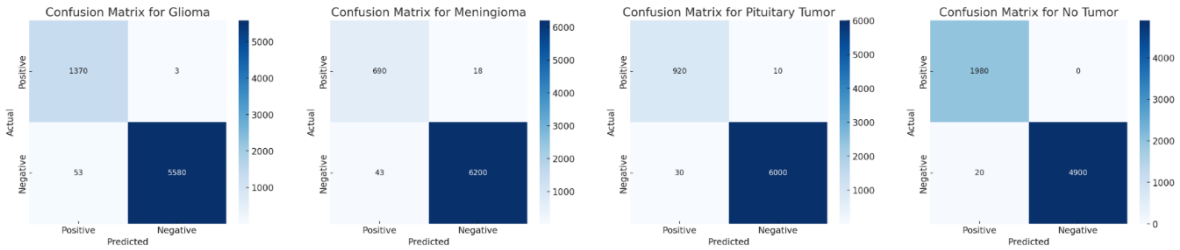

(a) (b) (c) (d)

Figure 4. The confusion matrix for the proposed models; (a) glioma, (b) meningioma, (c) pituitary tumor, and (d) no tumor

5. DISCUSSION

Compared to related works, the proposed novel hybrid model achieves superior accuracy, robustness, and interpretability. Its integration of precise segmentation and robust classification ensures improved performance over standalone or ensemble methods. The comparison between the proposed novel hybrid model and related works is summarized in Table 4.

The proposed hybrid U-Net and ResNet50 architecture has demonstrated exceptional performance in brain tumor classification, achieving an accuracy of 99.78±0.05%. By combining the segmentation power of U-Net with the classification capabilities of ResNet50, our model provides a robust solution for multi-class tumor classification, effectively handling complex cases such as glioma, meningioma, pituitary tumors, and no tumor with unparalleled precision. The use of a comprehensive Kaggle dataset with 7,023 images further underscores the reliability and scalability of the proposed approach. Among these [1], [3]-[6], [8], [14], [28]-[31] related works, none have achieved the level of accuracy or efficiency demonstrated by our novel hybrid model. For instance, models such as [14] 3D U-Net with radiomics (92.4%) and [8] hybrid grad-CAM with pre-trained models (97.4%) fell short in performance due to limitations in feature representation and dataset adaptability. Meanwhile, even high-performing models like [3] EfficientNetB2 (99.06%) and [6] MobileNetV2 with ensemble (99.38%) have been outperformed by our hybrid approach. This integration of advanced segmentation techniques and deep feature extraction solidifies the proposed model as a state-of-the-art solution, pushing the boundaries of brain tumor classification accuracy and efficiency.

In addition, a ViT model has been applied to MRI scan imagery, addressing four tumor classes but lacking clarity in image count and performance metrics [33]. Similarly, a hybrid deep learning model has been tested on a public MRI dataset for multi-class tumor recognition, but details on dataset size and accuracy remain unspecified [35]. Another effort utilizes an advanced deep learning framework across multi-institutional MRI datasets, showing high classification effectiveness though without quantifiable metrics [34]. More concretely, [32] using ResNet50, Xception, and MobileNetV2 achieved 99% accuracy on a 7,023-image public Kaggle MRI dataset. Building upon this, our proposed Hybrid U-Net and ResNet50 model not only employs efficient segmentation and classification integration but also surpasses previous methods with a classification accuracy of 99.78 ± 0.05%, demonstrating strong potential for real-world clinical decision support.

Table 4. The comparison between the proposed novel hybrid model and related works

Model	Year	Models	Dataset	Classes of tumors	Total images	Classification type	Acc. (%)
[28]	2022	CNN with NLCMFO	BRATS 2015	brain tumors	2,200	Binary	97.4
[1]	2022	Hybrid CNN-SVM	Hybrid dataset	Benign and malignant tumors	330	Binary	98.49
[3]	2023	EfficientNetB2	CE-MRI dataset	Glioma, meningioma, and pituitary tumors	3,064	Multi-class	99.06
[6]	2024	MobileNetV2 with Ensemble	Kaggle dataset	Binary and multi-class tumors	7,023	Binary and Multi-class	99.38
[14]	2024	3D U-Net with Radiomics	BRATS2021 and Radiomics dataset	Glioma subtypes	424	Multi-class	92.4
[29]	2024	DenseNet121 + InceptionV3	CE-MRI dataset	Glioma, meningioma, and pituitary tumors	3,064	Multi-class	95
[5]	2024	Customized CNN	Kaggle MRI dataset	Glioma, meningioma, pituitary tumor, and no tumor	7,023	Multi-class	99.02
[30]	2024	Res-BRNet	Br35H dataset	Glioma, meningioma, pituitary tumor, and no tumor	7,023	Multi-class	99
[4]	2024	ResNet50, Xception, InceptionV3	Figshare, SARTAJ, Br35H	Glioma, meningioma, pituitary tumor, and no tumor	7,023	Multi-class	99
[8]	2024	Hybrid Grad-CAM with pre-trained models	Kaggle dataset	Glioma, meningioma, pituitary tumor, and no tumor	7,023	Multi-class	97.4
[31]	2024	DenseNet + InceptionV3 Ensemble	Kaggle dataset	Glioma, meningioma, pituitary tumor, and no tumor	7,023	Multi-class	98.49
[33]	2024	ViT	MRI scan imagery dataset	Glioma, meningioma, pituitary, no tumor	Not specified	Multi-class	N/A
[35]	2024	Hybrid deep learning model	Public MRI Dataset	Glioma, meningioma, pituitary, and no tumor	Not specified	Multi-class	N/A
[34]	2025	Advanced deep learning framework	Multi-institution MRI dataset	Glioma, meningioma, pituitary, and no tumor	Not specified	Multi-class	N/A
[32]	2025	ResNet50, Xception, and MobileNetV2	Public Kaggle MRI dataset	Glioma, meningioma, pituitary, and no tumor	7,023	Multi-class	99
Our proposed		**Hybrid U-Net and ResNet50**	**Kaggle dataset**	**Glioma, meningioma, pituitary tumor, and no tumor**	**7,023**	**Multi-class**	**99.78 ± 0.05**

6. CONCLUSION

This paper presents a novel hybrid model combining U-Net for segmentation and ResNet50 architecture for classification, achieving state-of-the-art performance in brain tumor classification from MRI images. The proposed model attains an overall accuracy of 99.78±0.05%, significantly surpassing existing methods by integrating precise segmentation and robust classification. The U-Net component ensures accurate tumor boundary delineation, while ResNet50 delivers reliable multi-class classification across glioma, meningioma, pituitary tumor, and no tumor categories. The evaluation metrics and confusion matrix highlight the model's balanced performance, achieving accuracy exceeding 99% for all classes, with particularly outstanding results in the no tumor. By leveraging a diverse dataset of 7,023 images, the model demonstrates strong generalization and robustness. The proposed novel hybrid model sets a new benchmark for brain tumor classification, providing a reliable, accurate, and interpretable solution for medical imaging. Its advancements offer significant potential for real-world clinical applications and lay the groundwork for further innovations in brain tumor diagnostics.

Future research should focus on validating the model on multi-center datasets, enhancing interpretability through attention or explainability methods, and integrating uncertainty quantification to increase clinical trust. Furthermore, optimization for real-time deployment in clinical settings, especially on resource-constrained systems, is a promising direction to pursue.

ACKNOWLEDGMENTS

The authors gratefully acknowledge the support provided by Kalasin University for this work.

FUNDING INFORMATION

This research has not received any specific grant from funding agencies in the public, commercial, or not-for-profit sectors.

AUTHOR CONTRIBUTIONS STATEMENT

This journal uses the Contributor Roles Taxonomy (CRediT) to recognize individual author contributions, reduce authorship disputes, and facilitate collaboration.

Name of Author	C	M	So	Va	Fo	I	R	D	O	E	Vi	Su	P	Fu
Nattavut Sriwiboon	✓	✓	✓	✓	✓	✓	✓	✓	✓	✓	✓	✓	✓	✓
Songgrod Phimphisan	✓	✓		✓						✓	✓	✓	✓	✓

C : **C**onceptualization
M : **M**ethodology
So : **So**ftware
Va : **Va**lidation
Fo : **Fo**rmal analysis
I : **I**nvestigation
R : **R**esources
D : **D**ata Curation
O : Writing - **O**riginal Draft
E : Writing - Review & **E**diting
Vi : **Vi**sualization
Su : **Su**pervision
P : **P**roject administration
Fu : **Fu**nding acquisition

CONFLICT OF INTEREST STATEMENT

The authors declare that they have no conflict of interest.

INFORMED CONSENT

We have obtained informed consent from all individuals included in this study.

ETHICAL APPROVAL

This study does not involve human participants or animals; therefore, ethical approval is not required.

DATA AVAILABILITY

The data that support the findings of this study are publicly available from the Kaggle repository at Brain Tumor MRI Dataset (https://www.kaggle.com/datasets/masoudnickparvar/brain-tumor-mri-dataset). The dataset contains brain MRI images categorized into four classes (glioma, meningioma, pituitary tumor, and no tumor) and is intended for research in medical image analysis and deep learning.

REFERENCES

[1] M. O. Khairandish, M. Sharma, V. Jain, J. M. Chatterjee, and N. Z. Jhanjhi, "A Hybrid CNN-SVM Threshold Segmentation Approach for Tumor Detection and Classification of MRI Brain Images," *IRBM*, vol. 43, no. 4, pp. 290-299, 2022, doi: 10.1016/j.irbm.2021.06.003.

[2] B. Lu *et al.*, "A practical Alzheimer's disease classifier via brain imaging-based deep learning on 85,721 samples," *Journal of Big Data*, vol. 9, no. 1, p. 101, 2022, doi: 10.1186/s40537-022-00650-y.

[3] B. B. Vimala, S. Srinivasan, S. K. Mathivanan, Mahalakshmi, P. Jayagopal, and G. T. Dalu, "Detection and classification of brain tumor using hybrid deep learning models," *Scientific Reports*, vol. 13, no. 1, p. 23029, Dec 27 2023, doi: 10.1038/s41598-023-50505-6.

[4] E. Albalawi *et al.*, "Enhancing brain tumor classification in MRI scans with a multi-layer customized convolutional neural network approach," *Frontiers in Computational Neuroscience*, vol. 18, p. 1418546, 2024, doi: 10.3389/fncom.2024.1418546.

[5] K. M. Hosny, M. A. Mohammed, R. A. Salama, and A. M. Elshewey, "Explainable ensemble deep learning-based model for brain tumor detection and classification," *Neural Computing and Applications*, vol. 37, pp. 1289-1306, 2024, doi: 10.1007/s00521-024-10401-0.

[6] S. M, B. Bv, P. D, A. K. S, S. K. Mathivanan, and M. A. Shah, "Efficient brain tumor grade classification using ensemble deep learning models," *BMC Medical Imaging*, vol. 24, no. 1, p. 297, 2024, doi: 10.1186/s12880-024-01476-1.

[7] M. S. Salih and A. A. Mohsin, "A Fusion-Based Deep Approach for Enhanced Brain Tumor Classification," *Journal of Soft Computing and Data Mining*, vol. 5, no. 1, pp. 183-193, 2024.

[8] M. M. Zahoor *et al.*, "Brain Tumor MRI Classification Using a Novel Deep Residual and Regional CNN," *Biomedicines*, vol. 12, no. 7, Jun 23 2024, doi: 10.3390/biomedicines12071395.

[9] D. Dani, G. Agrawal, A. Kumaresan, and J. Thangarasu, "Multi-Class Classification and Feature Selection-Based Brain Tumor Detection Using Fast Point Dual-Channel Attention-Based Convolutional Neural Networks," *Biomedical Materials & Devices*, vol. 4, pp. 977–997, 2026, doi: 10.1007/s44174-025-00377-3.

[10] A. Hekmat, Z. Zhang, S. U. Rehman Khan, and O. Bilal, "Brain tumor diagnosis redefined: Leveraging image fusion for MRI enhancement classification," *Biomedical Signal Processing and Control*, vol. 109, p. 108040, 2025, doi: 10.1016/j.bspc.2025.108040.
[11] A. Berger, "Magnetic resonance imaging," *BMJ*, vol. 324, no. 7328, p. 35, Jan 5 2002, doi: 10.1136/bmj.324.7328.35.
[12] Y. Ji *et al.*, "Exploring functional dysconnectivity in schizophrenia: alterations in eigenvector centrality mapping and insights into related genes from transcriptional profiles," *Schizophrenia*, vol. 10, no. 1, p. 37, 2024, doi: 10.1038/s41537-024-00457-1.
[13] A. Kanyal *et al.*, "Multi-modal deep learning from imaging genomic data for schizophrenia classification," *Frontiers in Psychiatry*, vol. 15, 2024, doi: 10.3389/fpsyt.2024.1384842.
[14] X. Sun *et al.*, "Glioma subtype prediction based on radiomics of tumor and peritumoral edema under automatic segmentation," *Scientific Reports*, vol. 14, no. 1, p. 27471, Nov 10 2024, doi: 10.1038/s41598-024-79344-9.
[15] A. Rahman *et al.*, "Deep learning-driven segmentation of ischemic stroke lesions using multi-channel MRI," *Biomedical Signal Processing and Control*, vol. 105, p. 107676, 2025, doi: 10.1016/j.bspc.2025.107676.
[16] N. B. Vikhe and M. Shrivastava, "White Headed Timber Optimization based Deep Learning model for Brain Tumor Prediction," *Biomedical Materials & Devices*, vol. 4, pp. 2072–2096, 2026, doi: 10.1007/s44174-025-00293-6.
[17] C. H. Salh and A. M. Ali, "Automatic detection of breast cancer for mastectomy based on MRI images using Mask R-CNN and Detectron2 models," *Neural Computing and Applications*, vol. 36, no. 6, pp. 3017-3035, 2024, doi: 10.1007/s00521-023-09237-x.
[18] F. Kutlu, İ. Ayaz, and H. Garg, "Integrating fuzzy metrics and negation operator in FCM algorithm via genetic algorithm for MRI image segmentation," *Neural Computing and Applications*, vol. 36, no. 27, pp. 17057-17077, 2024, doi: 10.1007/s00521-024-09994-3.
[19] C. Guida, M. Zhang, and J. Shan, "Improving knee osteoarthritis classification using multimodal intermediate fusion of X-ray, MRI, and clinical information," *Neural Computing and Applications*, vol. 35, no. 13, pp. 9763-9772, 2023, doi: 10.1007/s00521-023-08214-8.
[20] X. Pan *et al.*, "Spatiotemporal context feedback bidirectional attention network for breast cancer segmentation based on DCE-MRI," *Neural Computing and Applications*, 2024, doi: 10.1007/s00521-024-10528-0.
[21] M. A. Nielsen, *Neural Networks and Deep Learning*. San Francisco: Determination Press, 2015.
[22] N. Sriwiboon, "Explainable artificial intelligence (XAI) for efficient lung cancer diagnosis using transformer–CNN hybrid with metadata fusion," *Neural Computing and Applications*, vol. 38, no. 3, p. 38, 2026, doi: 10.1007/s00521-025-11791-5.
[23] S. Rashmi, S. Srinath, R. Rakshitha, and B. V. Poornima, "Ensemble learning methods with single and multi-model deep learning approaches for cephalometric landmark annotation," *Discover Artificial Intelligence*, vol. 4, no. 1, p. 93, 2024, doi: 10.1007/s44163-024-00207-3.
[24] K. L. Arega, K. K. Tune, A. M. Beyene, W. Tariku, and N. M. Bune, "A review of deep-learning-based models for afaan oromo fake news detection on social media networks," *Discover Artificial Intelligence*, vol. 5, no. 1, p. 190, 2025, doi: 10.1007/s44163-025-00306-9.
[25] S. Nie, "Dynamic prediction and recommendation of museum visitors' interest based on long short-term memory network (LSTM)," *Discover Artificial Intelligence*, vol. 5, no. 1, p. 216, 2025, doi: 10.1007/s44163-025-00472-w.
[26] Y. Nie, K. H. Yu, Y. Wang, and P. Liu, "Applications of machine learning and deep learning in hydrology from a bibliometric perspective: a comprehensive review," *Discover Artificial Intelligence*, vol. 5, no. 1, p. 242, 2025, doi: 10.1007/s44163-025-00471-x.
[27] I. Goodfellow, Y. Bengio, and A. Courville, *Convolutional Neural Networks (CNNs)*. Cambridge, MA: MIT Press, 2016, pp. 326-359.
[28] A. A. Dehkordi, M. Hashemi, M. Neshat, S. M. Mirjalili, and A. S. Sadiq, "Brain Tumor Detection and Classification Using a New Evolutionary Convolutional Neural Network," *ArXiv*, 2022, doi: 10.48550/arXiv.2204.12297.
[29] D. E. Imbaquingo-Esparza, M. Botto-Tobar, J. G. Jacome-Leon, and M. Zambrano-Vizuete, "Exploring Advanced Deep Learning Paradigms for Precise Brain Tumor Categorization," *SN Computer Science*, vol. 5, no. 7, p. 965, 2024, doi: 10.1007/s42979-024-03228-y.
[30] H. Fakhri, S. Setiawardhana, I. Syarif, and R. Sigit, "Klasifikasi Tumor Otak Menggunakan Convolutional Neural Network," *Jurnal Inovtek Polbeng - Seri Informatika*, vol. 9, no. 1, 2024-06-16 2024, doi: 10.35314/isi.v9i1.3908.
[31] Z. Li and O. Dib, "Empowering Brain Tumor Diagnosis through Explainable Deep Learning," *Machine Learning and Knowledge Extraction*, vol. 6, pp. 2248-2281, 2024, doi: 10.3390/make6040111.
[32] R. Disci, F. Gurcan, and A. Soylu, "Advanced Brain Tumor Classification in MR Images Using Transfer Learning and Pre-Trained Deep CNN Models," *Cancers*, vol. 17, no. 1, p. 121doi: 10.3390/cancers17010121.
[33] C. K. K. Reddy *et al.*, "A fine-tuned vision transformer based enhanced multi-class brain tumor classification using MRI scan imagery," *Frontiers in Oncology*, vol. 14, p. 1400341, 2024, doi: 10.3389/fonc.2024.1400341.
[34] R. B. Vure and L. K. Pappala, "Enhanced brain tumor classification framework using deep learning," *Scientific Reports*, vol. 15, no. 1, p. 35814, 2025, doi: 10.1038/s41598-025-19882-y.
[35] M. M. Ahmed *et al.*, "Brain tumor detection and classification in MRI using hybrid ViT and GRU model with explainable AI in Southern Bangladesh," *Scientific Reports*, vol. 14, no. 1, p. 22797, 2024, doi: 10.1038/s41598-024-71893-3.
[36] O. Ronneberger, P. Fischer, and T. Brox, "U-Net: Convolutional Networks for Biomedical Image Segmentation," in *International Conference on Medical Image Computing and Computer-Assisted Intervention*, 2015, pp 234–241, doi: 10.1007/978-3-319-24574-4_28.
[37] K. He, X. Zhang, S. Ren, and J. Sun, "Deep Residual Learning for Image Recognition," in *2016 IEEE Conference on Computer Vision and Pattern Recognition (CVPR)*, Las Vegas, NV, USA, 2016, pp. 770-778, doi: 10.1109/CVPR.2016.90.
[38] J. Xu, J. Wan, and X. Zhang, "MD-TransUNet: TransUNet with Multi-attention and Dilated Convolution for Brain Stroke Lesion Segmentation," in *International Conference on Collaborative Computing: Networking, Applications and Worksharing*, Cham: Springer Nature Switzerland, pp. 151-170, doi: 10.1007/978-3-031-54528-3_9.
[39] M. L. F. Jumaili and E. Sonuç, "ML-Driven Alzheimer's disease prediction: A deep ensemble modeling approach," *SLAS Technology*, vol. 32, p. 100298, 2025, doi: 10.1016/j.slast.2025.100298.
[40] S. U. R. Khan, S. Asif, and O. Bilal, "Ensemble Architecture of Vision Transformer and CNNs for Breast Cancer Tumor Detection From Mammograms," *International Journal of Imaging Systems and Technology*, vol. 35, no. 3, p. e70090, 2025, doi: 10.1002/ima.70090.
[41] M. Kumari, G. Singh, and S. D. Pande, "A Survey of Current Progress in Depression Detection Using Deep Learning and Machine Learning," *Biomedical Materials & Devices*, 2025, doi: 10.1007/s44174-025-00301-9.
[42] P. Krishnaleela and R. M. Prakash, "CNN-SLSTM framework for human activity recognition using wearable sensor data," *Neural Computing and Applications*, vol. 4, pp. 716–740, 2026, doi: 10.1007/s00521-025-11410-3.

[43] H. Kibriya, A. Siddiqa, and W. Z. Khan, "Melanoma lesion localization using UNet and explainable AI," *Neural Computing and Applications*, vol. 37, pp. 10175–10196, 2025, doi: 10.1007/s00521-025-11080-1.
[44] M. A. Khan, R. Hamila, and H. Menouar, "Accelerating deep learning with fixed time budget," *Neural Computing and Applications*, vol. 37, no. 6, pp. 4869-4879, 2025, doi: 10.1007/s00521-024-10637-w.
[45] H. Zhang, Y. Zhang, J. Zhang, X. Meng, and J. Sun, "Resilient dispatching optimization of power system driven by deep reinforcement learning model," *Discover Artificial Intelligence*, vol. 5, no. 1, p. 189, 2025, doi: 10.1007/s44163-025-00451-1.
[46] Y. Moreno-Alcayde, T. Ruotsalo, L. A. Leiva, and V. J. Traver, "Affective annotation of videos from EEG-based crowdsourcing," *Pattern Analysis and Applications*, vol. 28, no. 3, p. 146, 2025, doi: 10.1007/s10044-025-01476-z.
[47] D. Liu *et al*., "SCAU-net: 3D self-calibrated attention U-Net for brain tumor segmentation," *Neural Computing and Applications*, vol. 35, no. 33, pp. 23973-23985, 2023, doi: 10.1007/s00521-023-08872-8.
[48] H. H. Khan and M. I. Khan, "An optimized deep focused U-Net model for image segmentation," *Neural Computing and Applications*, vol. 37, pp. 9245–9271, 2024, doi: 10.1007/s00521-024-10417-6.
[49] V. C. Joshi, M. A. Mehta, and K. Kotecha, "White blood cell segmentation using U-Net and its variants to improve leukemia diagnosis," *Neural Computing and Applications*, vol. 37, pp. 3265–3286, 2024, doi: 10.1007/s00521-024-10757-3.
[50] J. Liu, T. Zhang, Y. Kang, J. Qiang, D. Hu, and Y. Zhang, "SureUnet: sparse autorepresentation encoder U-Net for noise artifact suppression in low-dose CT," *Neural Computing and Applications*, vol. 37, pp. 7561–7573, 2023, doi: 10.1007/s00521-023-08847-9.
[51] T. Hussain, H. Shouno, M. A. Mohammed, H. A. Marhoon, and T. Alam, "DCSSGA-UNet: Biomedical image segmentation with DenseNet channel spatial and Semantic Guidance Attention," *Knowledge-Based Systems*, vol. 314, p. 113233, 2025, doi: 10.1016/j.knosys.2025.113233.
[52] S. Sulaiman, M. R. Thanka, E. B. Edwin, and N. Salam, "Adaptive Neuro Transformers for Stroke Lesion Segmentation: GatedNeuroTransUNet Implemented using CNNs with Bottleneck Residual Blocks," *SN Computer Science*, vol. 6, no. 5, p. 492, 2025, doi: 10.1007/s42979-025-04026-w.
[53] J. Hu, L. Shen, and G. Sun, "Squeeze-and-Excitation Networks," in *Proceedings of the IEEE Conference on Computer Vision and Pattern Recognition (CVPR)*, Salt Lake City, UT, USA, 2018, pp. 7132-7141, doi: 10.1109/CVPR.2018.00745.
[54] D. Mahajan, R. Girshick, V. Ramanathan, K. He, M. Paluri, and Y. Li, "Exploring the Limits of Weakly Supervised Pretraining," in *Proceedings of the European Conference on Computer Vision (ECCV)*, 2018, pp. 181-196, doi: 10.1007/978-3-030-01216-8_12.
[55] H. Touvron, A. Vedaldi, M. Douze, and H. Jégou, "Fixing the Train-Test Resolution Discrepancy," in *Proceedings of the 33rd International Conference on Neural Information Processing Systems*, pp. 11410-11420, 2019, doi: 10.5555/3454287.3455028.
[56] T. R. Jeyalakshmi, S. M. Karthik, and S. Karunya, "Enhanced Pulmonary Embolism Detection in CT Angiography Using Spectral ResNet Hyper Convolutional Neural Network," *SN Computer Science*, vol. 5, no. 8, p. 1041, 2024, doi: 10.1007/s42979-024-03352-9.
[57] H. Rabie and M. A. Akhloufi, "A review of machine learning and deep learning for Parkinson's disease detection," *Discover Artificial Intelligence*, vol. 5, no. 1, p. 24, 2025, doi: 10.1007/s44163-025-00241-9.
[58] L. Zhou and Y. Wang, "Brain tumor image segmentation based on shuffle transformer-dynamic convolution and inception dilated convolution," *Computer Vision and Image Understanding*, vol. 254, p. 104324, 2025, doi: 10.1016/j.cviu.2025.104324.
[59] Y. Yin, S. He, R. Zhang, H. Chang, and J. Zhang, "Deep learning for iris recognition: a review," *Neural Computing and Applications*, vol. 37, no. 17, pp. 11125-11173, 2025, doi: 10.1007/s00521-025-11109-5.
[60] M. Nickparvar, Brain Tumor MRI Dataset. Kaggle, 2024. [Online]. Available: https://www.kaggle.com/datasets/masoudnickparvar/brain-tumor-mri-dataset. (Accessed: Jan. 1, 2025).

BIOGRAPHIES OF AUTHORS

Nattavut Sriwiboon is Assistant Professor of Information Technology, Department of Computer Science and Information Technology, Kalasin University, Thailand. Received the Bachelor of Science degree in Computer Science from the Faculty of Informatics, Mahasarakham University, Thailand, in May 2009. He earned the Master of Science degree in Information Technology from the same institution in June 2012, he completed his Doctor of Philosophy in Computer Science from the Faculty of Informatics, Mahasarakham University, Thailand. His research interests include advanced deep learning techniques, medical image analysis, and computational efficiency optimization in neural networks. He can be contacted at email: nattavut.sr@ksu.ac.th.

Songgrod Phimphisan is Assistant Professor of Information Technology, Department of Computer Science and Information Technology, Kalasin University, Thailand. Received the Bachelor of Science degree in Computer Science from Mahidol University, Thailand, in 1996. He earned the Master of Science degree in Information Technology from King Mongkut's Institute of Technology Ladkrabang, Thailand, in 2003. In 2016, he completed his Doctor of Philosophy in Electrical and Computer Engineering at Mahasarakham University, Thailand. His research interests include computational intelligence, advanced information systems, and deep learning applications in engineering and technology. He can be contacted at email: songgrod.ph@ksu.ac.th.